APL Photonics

Invited Article: Four-mode semiconductor optical amplifier

Cite as: APL Photonics 1, 070801 (2016); https://doi.org/10.1063/1.4955178
Submitted: 01 April 2016 • Accepted: 22 June 2016 • Published Online: 01 August 2016

He Wen, Yousef Alahmadi, Patrick LiKamWa, et al.

COLLECTIONS

This paper was selected as an Editor's Pick

View Online Export Citation CrossMark

ARTICLES YOU MAY BE INTERESTED IN

Tutorial on narrow linewidth tunable semiconductor lasers using Si/III-V heterogeneous integration
APL Photonics 4, 111101 (2019); https://doi.org/10.1063/1.5124254

Active mode-locking via pump modulation in a Tm-doped fiber laser
APL Photonics 1, 071303 (2016); https://doi.org/10.1063/1.4965249

Single-mode optical waveguides on native high-refractive-index substrates
APL Photonics 1, 071302 (2016); https://doi.org/10.1063/1.4955065

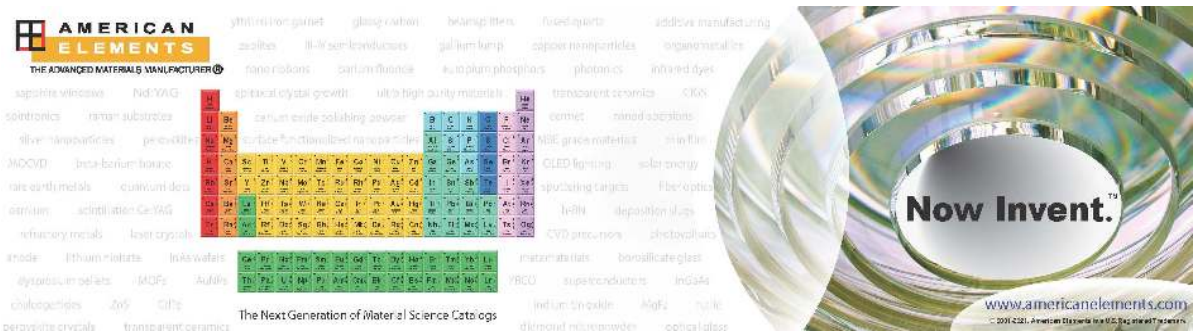

© 2016 Author(s).

Invited Article: Four-mode semiconductor optical amplifier

He Wen,[1,2,a] Yousef Alahmadi,[2,a] Patrick LiKamWa,[2] Cen Xia,[2] Christian Carboni,[2] and Guifang Li[1,2,b]
[1]*The College of Precision Instruments and Opto-Electronic Engineering, Tianjin University, Tianjin 300072, People's Republic of China*
[2]*CREOL, The College of Optics and Photonics, University of Central Florida, 4304 Scorpius St., Orlando, Florida 32816-2700, USA*

(Received 1 April 2016; accepted 22 June 2016; published online 1 August 2016)

We demonstrate the first few-mode semiconductor optical amplifier (FM SOA) that supports up to four waveguide modes. We show that each of the modes are confined to the waveguide, overlapping the quantum wells with approximately the same amount, leading to equalized gain for each of the four waveguide modes. © *2016 Author(s). All article content, except where otherwise noted, is licensed under a Creative Commons Attribution (CC BY) license (http://creativecommons.org/licenses/by/4.0/).* [http://dx.doi.org/10.1063/1.4955178]

The exponential growth in internet traffic in recent years has made clear the need for an infrastructure overhaul to address the shortcomings in available capacity provided by single mode fiber (SMF).[1] Currently, two approaches offer promising solutions to the "capacity crunch."[2,3] The first solution, multiple parallel wavelength division multiplexed (WDM) systems,[4,5] employing multiple coherent optical communication channels,[6] one on top of the other, does allow for multiplicative capacity scaling that would, in theory, provide as much capacity as needed. While this is a mature technology, it is not very economically attractive, as the cost of a parallel WDM system scales linearly with design capacity.[7] The second solution relies on the principles of space-division multiplexing (SDM) encompassing mode-division multiplexing (MDM) and core multiplexing.[8–13] The ultimate goal of SDM research is to replace parallel WDM systems into a single SDM system thereby reducing the cost per bit for optical transmission.

Integration is often a path way to cost reduction. In the case of SDM, integration of parallel fibers into a single SDM fiber may not offer significant saving as the majority of the cost of the fiber infrastructure comes from cabling and installation. Large-scale integration of transmitters and receivers could help reduce costs[7] but it is applicable to both parallel WDM systems and SDM system. So, it's clear that innovations in the individual components used in SDM will be the key. One of those components that may present such an opportunity is optical amplifiers.

Single-mode erbium-doped fiber amplifiers (EDFAs) can be reconfigured into few-mode (FM) EDFAs by replacing the input and erbium-doped SMFs of the EDFA with corresponding few-mode fibers (FMF). However, mode-dependent gain is rather large for such a simple extension.[14,15] To address this issue, a gain-equalized FM EDFA must be constructed by controlling the pump modal content[16–18] or erbium spatial distribution.[19] For example, for a 3-mode EDFA, gain equalization can be achieved using the LP_{11} mode as the forward pump, and pumping the LP_{02} mode in the backward direction.[16] While is indeed capable of delivering the desired equalized gain, but it contains approximately the same amount of components that three independent single-mode EDFAs would. Therefore, there would not be much cost savings over a parallel-WDM system utilizing independent SM EDFAs. Furthermore, interdependencies between modes make FM EDFA performance subpar to SM EDFAs.

The difficulty in engineering a gain-equalized EDFAs for SDM provide motivation for research into few-mode semiconductor optical amplifiers (FM SOA). FM SOAs have the potential to provide

[a]H. Wen and Y. Alahmadi contributed equally to this work.
[b]Electronic mail: Li@creol.ucf.edu.

 ©Author(s) 2016.

TABLE I. Epitaxial layer structure of FM-SOA.

Layer	Material	Thickness (nm)	Doping (cm^{-3})
P-contact	InGaAs	100	$P = 1.3\times10^{19}$
Top cladding	InP	1300	$P = 1.0\times10^{18}$
	InP	200	$P = 5.0\times10^{17}$
Etch control	InGaAsP(1.3Q)	50	Undoped
	InP	50	Undoped
	InGaAsP(1.3Q)	106	Undoped
3-QW/barrier	InGaAsP(1.61Q)/(1.3Q)	6×3/10×2	Undoped
	InGaAsP(1.3Q)	353	Undoped
1-QW	InGaAsP(1.61Q)	6	Undoped
	InGaAsP(1.3Q)	353	Undoped
3-QW/barrier	InGaAsP(1.61Q)/(1.3Q)	6×3/10×2	Undoped
	InGaAsP(1.3Q)	106	Undoped
	InP	200	$N = 5.0\times10^{17}$
Lower cladding	InP	1300	$N = 1.0\times10^{18}$
Substrate	InP		$N = 5.2\times10^{18}$

gain-equalized amplification for multiple input modes without the additional component complexity of the aforementioned multi-mode EDFA setups,[20] making them more economically appealing.

Our four-mode SOA has the familiar structure of a P-I-N diode. As shown in Table I, the top layer is P-doped, the middle layer is intrinsic, and the bottom layer and substrate are N-doped. In this configuration, the waveguide has an index of refraction of 3.3877 and thickness of 1.2 μm, the substrate and cladding have indices of 3.1659, and above the cladding is air. The cladding thickness is 1.6 μm. Optical modes are supported by a ridge waveguide structure, which consists of a 5 μm strip with the cladding removed everywhere else. These dimensions and the index distribution allow the waveguide to support four modes: E_{11}, E_{12}, E_{21}, and E_{22} where the first index indicates the number of lobes in the horizontal direction and the second index indicates the number of lobes in the vertical direction. Figure 1 illustrates the simulated mode profiles of the FM SOA, including the indices of refraction and the dimensions of the chip itself. Due to geometric asymmetry of the waveguide, the $1/e^2$ full width of the E_{11} mode is 5.2 μm in the x direction and 1 μm in the y direction. This mode aspect ratio does not match that of the LP_{01} mode in FMFs, leading to reduced coupling efficiency. Similar mismatches apply to high-order modes. This issue can be addressed by using the combination of an objective lens and a cylindrical lens.

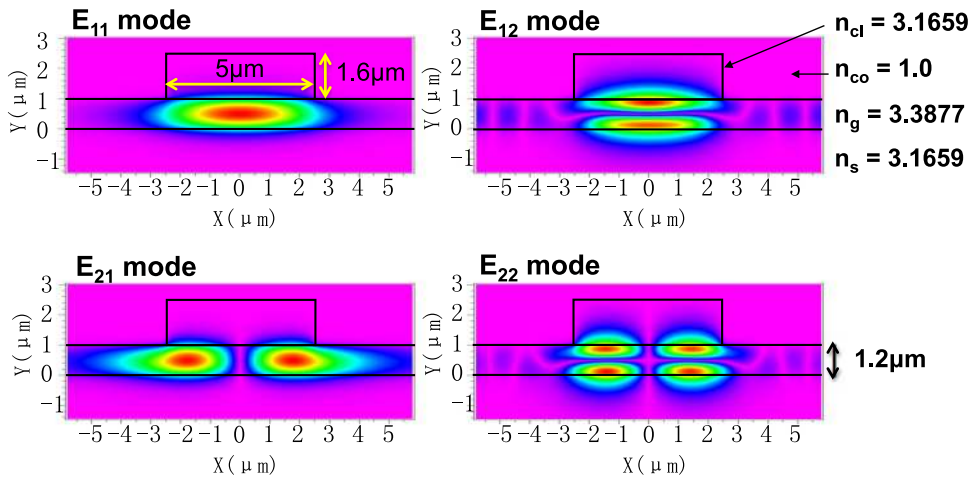

FIG. 1. Diagram of the index profile, dimensions and simulated mode profiles of the FM SOA.

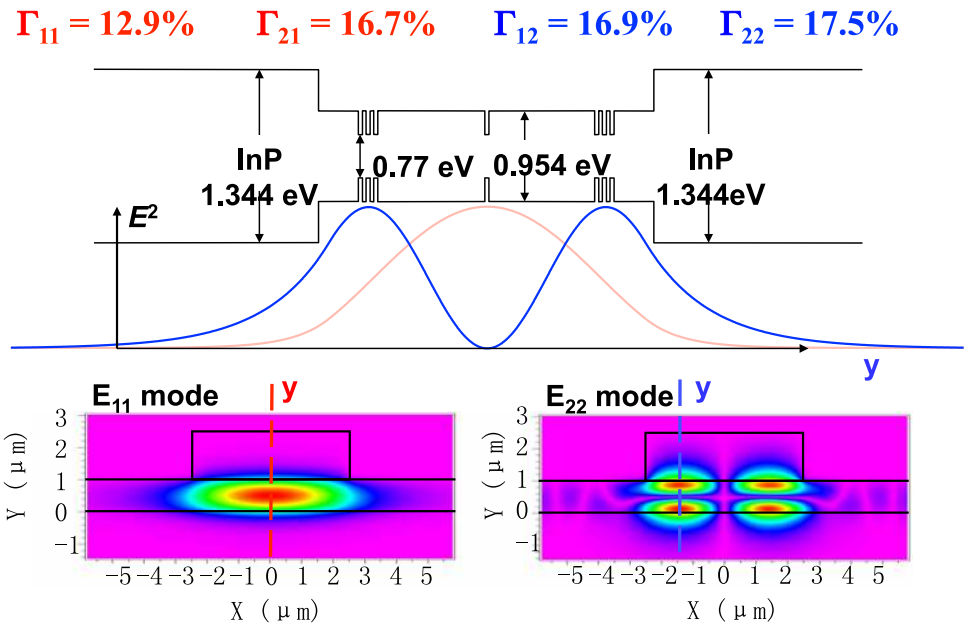

FIG. 2. Bandgap diagram and simulated mode profiles of the four-mode SOA demonstrating the strategic placement of the quantum wells to achieve similar overlap integrals for all four modes.

The P and N type layers have the same bandgap of 1.344 eV, while the intrinsic layer, where amplification occurs, is very rich and has a symmetric structure that contains seven strategically placed quantum wells. 200 nm down from the top layer resides the first group of three quantum wells with a thickness of 6 nm each, which have a bandgap of 0.77 eV, corresponding to a wavelength of 1.61 μm. The quantum wells in this group is separated by two 10 nm thick barrier layers, which have a bandgap of 0.954 eV, corresponding to a wavelength of approximately 1.3 μm. 350 nm further down from the first group of quantum wells resides a single quantum well of the same thickness and bandgap as those of the quantum wells found in the groups. Following this is a symmetrically constructed group of another three quantum wells. Figure 2 contains the bandgap diagram of our FM SOA.

The P-I-N diode is forward biased, causing the Fermi levels to split and allowing electrons and holes to occupy the quantum wells simultaneously. The quantum well regions are where the optical gain occurs, and therefore it is important that these be placed such that the overlap integrals between the waveguide modes and the quantum well regions are similar for all four modes. The calculated overlap integrals for the E_{11} and E_{21} modes, which have only one lobe in the vertical direction, are 12.9% and 16.7%, respectively. Similarly, the E_{12} and E_{22} modes have overlap integrals calculated to be 16.9% and 17.5%, respectively. Since all four modes have very similar confinement factors, they should experience very similar gains. Figure 2 illustrates the images of the waveguide modes superimposed onto the waveguide structure, and includes the position of the quantum wells, providing a very clear illustration of the strategic placement of the quantum wells such that all four modes have similar overlap integrals.

The fabrication of our FM SOA begins with a clean multi-quantum-well wafer. The ridge waveguide is then defined by first depositing a layer of SiO_2 film on top of the entire wafer using plasma-enhanced chemical vapor deposition and then delineating a 5 μm wide SiO_2 strip using contact-mask lithography and reactive-ion etching. The ridge waveguide is then created by wet etching, using the SiO_2 layer as a mask, down to the etch-stop layer – the very top of the intrinsic region. Once the waveguide has been formed, the top contact is formed by first spin coating the chip with BCB, which is fully cured in a nitrogen-only environment. The BCB film is thinned by reactive-ion etching until the very top of the waveguide is exposed, and the top electrode is created by depositing titanium, zinc, and gold using vacuum thermal air evaporation. Each top contact

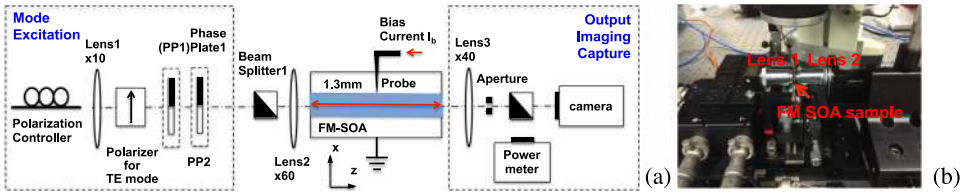

FIG. 3. (a) Schematic of the experimental setup used to characterize the SOA (Reproduced with permission from Proc. SPIE **9774**, 977406 (2016). Copyright 2016 Society of Photo Optical Instrumentation Engineers) and (b) an image of the actual setup.

is defined and isolated by photolithography and liftoff, as each chip is created to have multiple waveguide structures to be used independently. After thinning the sample down to approximately 200 μm and polishing it, the bottom contact is created by depositing nickel, germanium, and gold using thermal evaporation.

Figures 3(a) and 3(b) are a schematic and an image of the setup used to characterize the FM SOA. This setup is used to excite and image each waveguide mode individually. A polarization controller is used to ensure that only TE modes are excited, as the current SOA only exhibits waveguide gain for the TE polarization. The lens pair, consisting of a 10× and 60× lens, is used to transform the beam spot size from a SMF launch fiber to match the mode size of the SOA. We did not use the combination of an objective lens and a cylindrical lens because of its complexity. The difference between these two setups will be discussed later. In order to generate each of the modes, two phase plates are employed. If no phase plates are used, the E_{11} mode is excited. If only the horizontal phase plate is used, then the E_{12} mode is excited. Likewise, if only the vertical phase plate is used, then the E_{21} mode is excited. Finally, if both phase plates are used, the E_{22} mode is excited. Forward biasing of the FM SOA is accomplished by means of a probe, and a 40× microscope objective is used to magnify the output facet in order to image the mode profiles with a camera. The entire SOA is only 1.33 mm long. An aperture is used to spatially filter out the amplified spontaneous emission (ASE).

Images of the mode profiles with and without biasing can then be collected. Figures 4(a) and 4(b) are images of the mode profiles without any bias, and with a 40 mA bias, respectively. Clearly, all of the modes are intensified when the diode is biased, effectively confirming that the SOA does indeed induce optical gain.

Figure 5 is a plot of the on-off gain as a function of output power without amplification. As evident in Figure 5, the on-off gain is equalized for all four waveguide modes. However, the gain is significantly saturated to around 2 dB at high input power levels. This saturation also manifest in the amplified spontaneous emission (ASE) produced in the waveguide region. A comparison of the ASE output power versus bias current between our SOA and a commercially available chip of similar dimensions shows an approximately 25 dB lower ASE power for our device.

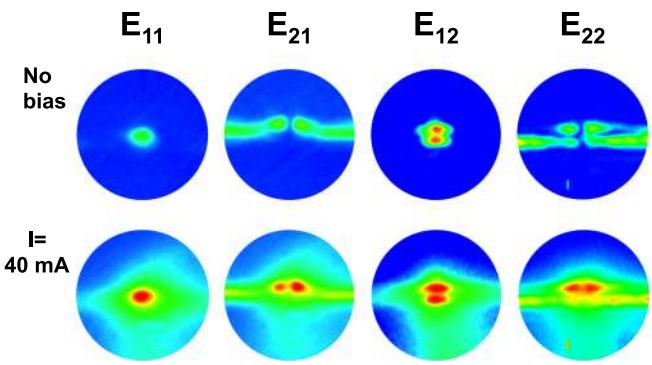

FIG. 4. Images of the actual FM SOA mode profiles (a) without bias and (b) with a 40 mA bias.

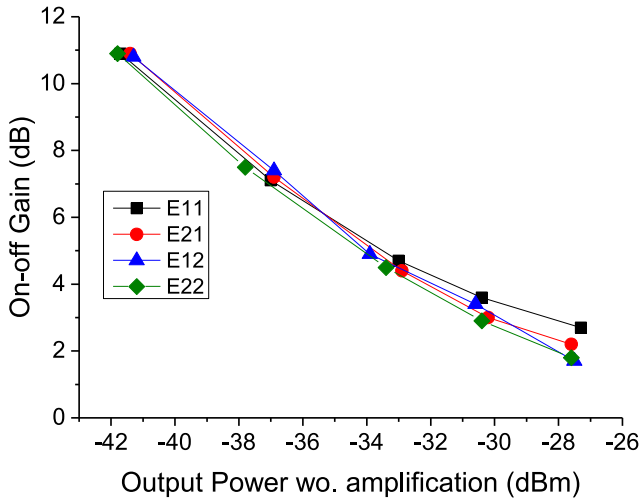

FIG. 5. On-off gain as a function of output power without amplification. Reproduced with permission from Proc. SPIE **9774**, 977406 (2016). Copyright 2016 Society of Photo Optical Instrumentation Engineers.

This reason for the low level of output power/amplification is because our current SOA has significant amounts of electronic and optical leakage. Figure 6 shows the four amplified SOA mode profiles without the aforementioned spatial aperture. As can be seen in Figure 6, in addition to the desired ridge waveguide modes, the chip supports slab waveguide modes that can be excited from amplified spontaneous emission. The existence of the slab mode was also predicted in simulation as shown in Fig. 1. The fact that both ridge waveguide mode and slab mode exist indicates that these modes have nearly the same propagation constant. According to simulations, the effective refractive indices 3.341, 3.221, 3.336, 3.213 for the E_{11}, E_{12}, E_{21}, E_{22} modes are close to that of the first-order slab mode at 3.334 in this device. High-order guided modes are easier to be coupled into the first-order slab mode because of weaker confinement in the horizontal direction. Another reason for low output power is that injected carriers can leak into the intrinsic slab region not under the ridge. This is because the spontaneous emission has a relatively slow recombination rate;[21] therefore, the

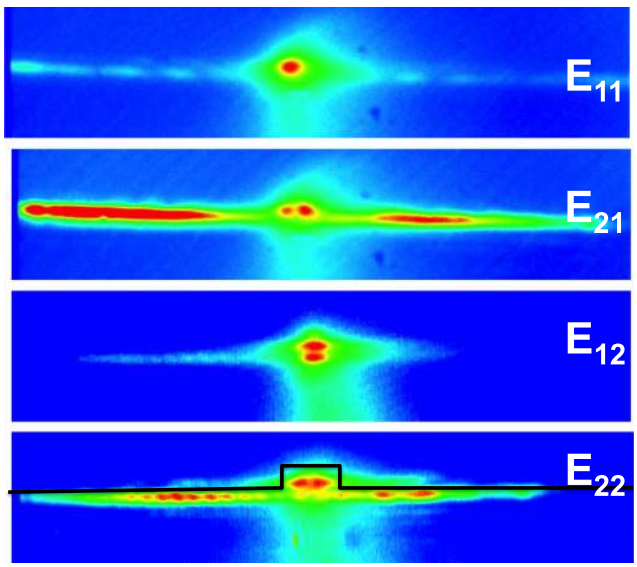

FIG. 6. Images of the four modes of our FM SOA with the dimensions of the waveguide superimposed over the image of the E_{22} mode.

electrons have a long lifetime, allowing them to leak into the 1 μm-high slab. The solution to these problems is to block the mode coupling and carrier leakage by etching deeper into the intrinsic layer when fabricating the SOAs. This approach has been verified by simulation and the results will be published in future.

To investigate the effect of the mismatch of aspect ratios on the coupling efficiency between the FMF and FM SOA given, we calculated the overlaps between these two groups of modes after suitable magnifications. Two scenarios were considered. First is equal magnification in horizontal and vertical directions, as in the case of our experiment using a pair of objective lenses. The second is unequal magnification realized by using of the combination an objective lens and a cylindrical lens. The coupling matrices for these two cases when the magnifications were optimized to maximize the coupling efficiency for the fundamental mode are as follows:

$$\begin{bmatrix} -2.67 & -49.3 & -50.7 & -41.9 \\ -64.2 & -4.32 & -49.8 & -66.1 \\ -53.3 & -54.5 & -4.23 & -43.3 \\ -92.0 & -64.8 & -45.9 & -4.18 \end{bmatrix}_{eq} \text{dB}, \quad \begin{bmatrix} -0.12 & -38.8 & -48.6 & -51.5 \\ -42.6 & -0.28 & -45.7 & -62.6 \\ -49.4 & -50.7 & -0.32 & -27.5 \\ -84.3 & -60.2 & -33.7 & -0.40 \end{bmatrix}_{uneq} \text{dB}.$$

The subscript denotes equal magnification or unequal magnification. The first to the last numbers in diagonal correspond to overlap integrals between E_{11} and LP_{01}, E_{12} and LP_{11b}, E_{21} and LP_{11a}, E_{22} and LP_{21a}. The non-diagonal element (i,j) represents mode crosstalk from mode j to mode i, where i denotes E_{11}, E_{12}, E_{21}, and E_{22}, j denotes LP_{01}, LP_{11b}, LP_{11a} and LP_{21a}. Perfect alignment without any offset is assumed.

We can see that the mismatch in aspect ratios reduces the coupling efficiency (diagonal elements) in the equal magnification case while the coupling efficiency reaches near unity if we employ mode-shape matching using unequal magnification. Mode crosstalk levels (off-diagonal elements) are low for both cases. This is because all modes are either symmetric (E_{11}) or antisymmetric (E_{12}, E_{21} and E_{22}). The overlap integrals of different modes in active region are negligible if there were no misalignments. But in experiments, unavoidable misalignments would increase mode crosstalk. The mode profiles of FW SOAs have better overlap with those of few-mode elliptical core fibers,[22,23] in comparison with circular FMFs, due to better match of the aspect ratios.

We successfully demonstrated the first few-mode semiconductor optical amplifier, supporting up to four waveguide modes. The chip was carefully designed and the quantum wells were strategically placed in the intrinsic layer to allow for equalized gain for all four modes with uniform pumping. Although this "proof of concept" FM SOA was fully functional, many improvements can be made to the design and fabrication in order to achieve less optical and electrical leakage. In the future, we intend to fabricate FM SOAs that are not polarization dependent, by using strained quantum wells. Furthermore, we intend to control the horizontal placement of the quantum wells by using selective area growth and quantum well intermixing. We envision FM SOAs will not only find applications in SDM but also many of the linear and nonlinear optical phenomena that we explored in single-mode SOAs.[24–26]

This work has been supported in part by the National Basic Research Program of China (973) Project No. 2014CB340104/3, NSFC Project Nos. 61377076, 61307085, and 61335005.

[1] R.-J. Essiambre, G. J. Foschini, G. Kramer, and P. J. Winzer, "Capacity limits of information transport in fiber-optic networks," Phys. Rev. Lett. **101**(16), 163901 (2008).
[2] A. Chraplyvy, presented at the 35th European Conference on Optical Communication, ECOC '09, 2009.
[3] D. J. Richardson, "Filling the light pipe," Science **330**(6002), 327–328 (2010).
[4] C. A. Brackett, "Dense wavelength division multiplexing networks: Principles and applications," IEEE J. Sel. Areas Commun. **8**(6), 948–964 (1990).
[5] T. Li, "The impact of optical amplifiers on long-distance lightwave telecommunications," Proc. IEEE **81**, 1568–1579 (1993).
[6] X. Li, X. Chen, G. Goldfarb, E. Mateo, I. Kim, F. Yaman, and G. Li, "Electronic post-compensation of WDM transmission impairments using coherent detection and digital signal processing," Opt. Express **16**(2), 880–888 (2008).
[7] P. J. Winzer, "Energy-efficient optical transport capacity scaling through spatial multiplexing," IEEE Photonics Technol. Lett. **23**(13), 851–853 (2011).
[8] P. J. Winzer, "Optical networking beyond WDM," IEEE Photonics J. **4**, 647–651 (2012).
[9] D. Richardson, J. Fini, and L. Nelson, "Space-division multiplexing in optical fibres," Nat. Photonics **7**, 354–362 (2013).

[10] G. Li, N. Bai, N. Zhao, and C. Xia, "Space-division multiplexing: The next frontier in optical communication," Adv. Opt. Photonics **6**(4), 1–75 (2014).
[11] Y. Kokubun and M. Koshiba, "Novel multi-core fibers for mode division multiplexing: Proposal and design principle," IEICE Electron. Exp. **6**, 522–528 (2009).
[12] R. Ryf, S. Randel, A. H. Gnauck, C. Bolle, R.-J. Essiambre, P. J. Winzer, D. W. Peckham, A. McCurdy, and R. Lingle, "Space-division multiplexing over 10 km of three-mode fiber using coherent 6×6 MIMO processing," in Proceedings of Optical Fiber Communication, PDP10, 2011.
[13] E. Ip, M.-J. Li, K. Bennett, Y.-K. Huang, A. Tanaka, A. Korolev, K. Koreshkov, W. Wood, E. Mateo, J. Hu, and Y. Yano, "$146\,\lambda \times 6 \times 19$-Gbaud wavelength-and mode-division multiplexed transmission over 10×50-km spans of few-mode fiber with a gain-equalized few-mode EDFA," J. Lightwave Technol. **32**(4), 790–797 (2014).
[14] E. Desurvire, *Erbium-Doped Fibre Amplifiers: Principles and Applications* (John Wiley, New York, 1994).
[15] Y. Jung, S. Alam, Z. Li, A. Dhar, D. Giles, I. Giles, J. Sahu, F. Poletti, L. Grüner-Nielsen, and D. Richardson, "First demonstration and detailed characterization of a multimode amplifier for space division multiplexed transmission systems," Opt. Express **19**(26), B952–B957 (2011).
[16] N. Bai, E. Ip, T. Wang, and G. Li, "Multimode fiber amplifier with tunable modal gain using a reconfigurable multimode pump," Opt. Express **19**(17), 16601–16611 (2011).
[17] E. Ip, N. Bai, Y. Huang, E. Mateo, F. Yaman, S. Bickham, H. Tam, C. Lu, M. Li, S. Ten, A. P. T. Lau, V. Tse, G. Peng, C. Montero, X. Prieto, and G. Li, "$88 \times 3 \times 112$-Gb/s WDM transmission over 50-km of three-mode fiber with inline multimode fiber amplifier," in *37th European Conference and Exposition on Optical Communications, OSA Technical Digest (CD)* (Optical Society of America, 2011), paper Th.13.C.2.
[18] Y. Jung, E. L. Lim, Q. Kang, T. C. May-Smith, N. H. L. Wong, R. Standish, F. Poletti, J. K. Sahu, S. U. Alam, and D. J. Richardson, "Cladding pumped few-mode EDFA for mode division multiplexed transmission," Opt. Express **22**(23), 29008–29013 (2014).
[19] G. Le Cocq, L. Bigot, A. Le Rouge, M. Bigot-Astruc, P. Sillard, C. Koebele, M. Salsi, and Y. Quiquempois, "Modeling and characterization of a few-mode EDFA supporting four mode groups for mode division multiplexing," Opt. Express **20**(24), 27051–27061 (2012).
[20] H. Wen, Y. Alahmadi, P. LiKamwa, C. Xia, C. Carboni, and G. Li, "Four-mode semiconductor optical amplifier," Proc SPIE **9774**, 977406 (2016).
[21] J. T. Verdeyen, *Laser Electronics*, 3rd ed. (Prentice Hall, Englewood, NJ, 1995).
[22] G. Milione, E. Ip, M. Li, J. Stone, G. Peng, and T. Wang, "Spatial mode analysis of an elliptical-core, few-mode, optical fiber for MIMO-less space-division-multiplexing," in *Optical Fiber Communication Conference* (Optical Society of America, 2016), paper W1F.3.
[23] E. Ip, G. Milione, M.-J. Li, N. Cvijetic, K. Kanonakis, J. Stone, G. Peng, X. Prieto, C. Montero, V. Moreno, and J. Liñares, "SDM transmission of real-time 10GbE traffic using commercial SFP + transceivers over 0.5 km elliptical-core few-mode fiber," Opt. Express **23**, 17120–17126 (2015).
[24] N. A. O'Mahony, "Semiconductor laser optical amplifiers for use in future fiber systems," J. Lightwave Technol. **6**(4), 531–544 (1988).
[25] A. Borghesani, "Semicounductor optical amplifiers for advanced optical applications," in Proceedings of International Conference on Transparent Optical Networks, Tu.C1.3, 2006.
[26] K. E. Stubkjaer, "Semiconductor optical amplifier-based all-optical gates for high-speed optical processing," IEEE J. Sel. Top. Quantum Electron. **6**(6), 1428–1435 (2000).